MOLECULAR AND CELLULAR BIOLOGY, Aug. 1998, p. 4761–4771 Vol. 18, No. 8
0270-7306/98/$04.00+0

RhoE Regulates Actin Cytoskeleton Organization and Cell Migration

ROSA M. GUASCH,[1,2] PETER SCAMBLER,[3] GARETH E. JONES,[2] AND ANNE J. RIDLEY[1,4]*

The Ludwig Institute for Cancer Research, London W1P 8BT,[1] Muscle and Motility Research Centre, The Randall Institute, King's College London, London, WC2B 5RL,[2] Institute of Child Health, London, WC1N 1EH,[3] and Department of Biochemistry and Molecular Biology, University College London, London WC1E 6BT,[4] United Kingdom

Received 29 December 1997/Returned for modification 5 February 1998/Accepted 3 May 1998

The actin cytoskeleton is regulated by Rho family proteins: in fibroblasts, Rho mediates the formation of actin stress fibers, whereas Rac regulates lamellipodium formation and Cdc42 controls filopodium formation. We have cloned the mouse *RhoE* gene, whose product is a member of the Rho family that shares (except in one amino acid) the conserved effector domain of RhoA, RhoB, and RhoC. RhoE is able to bind GTP but does not detectably bind GDP and has low intrinsic GTPase activity compared with Rac. The role of RhoE in regulating actin organization was investigated by microinjection in Bac1.2F5 macrophages and MDCK cells. In macrophages, RhoE induced actin reorganization, leading to the formation of extensions resembling filopodia and pseudopodia. In MDCK cells, RhoE induced the complete disappearance of stress fibers, together with cell spreading. However, RhoE did not detectably affect the actin bundles that run parallel to the outer membranes of cells at the periphery of colonies, which are known to be dependent on RhoA. In addition, RhoE induced an increase in the speed of migration of hepatocyte growth factor/scatter factor-stimulated MDCK cells, in contrast to the previously reported inhibition produced by activated RhoA. The subcellular localization of RhoE at the lateral membranes of MDCK cells suggests a role in cell-cell adhesion, as has been shown for RhoA. These results suggest that RhoE may act to inhibit signalling downstream of RhoA, altering some RhoA-regulated responses, such as stress fiber formation, but not affecting others, such as peripheral actin bundle formation.

Rho family proteins consist of 11 mammalian members, in addition to many homologs in other species, and form a subgroup of the Ras GTPases (40). Over the past few years, members of the Rho family have been implicated in many different cellular events, including actin organization, cell adhesion, membrane trafficking, and transcriptional regulation (52). Like all members of the Ras superfamily, they function as molecular switches, cycling between an active GTP-bound form and an inactive GDP-bound form (recently reviewed in reference 52). This property is determined by five primary sequence motifs that are highly conserved evolutionarily among members of the Ras superfamily (6). The activity of Rho GTPases is determined by the ratio of their GTP-bound and GDP-bound states and is regulated by the opposing effects of guanine nucleotide exchange factors, which enhance the exchange of bound GDP for bound GTP, and the GTPase-activating proteins (GAPs), which increase the intrinsic rate of hydrolysis of bound GTP. In addition, guanine nucleotide dissociation inhibitors can inhibit both the exchange of nucleotides and the hydrolysis of bound GTP (4).

Rho, Rac, and Cdc42 are three members of the Rho family known to be involved in regulating the organization of the actin cytoskeleton. In Swiss 3T3 fibroblasts, Rho regulates the formation of actin stress fibers, whereas Rac regulates lamellipodium formation and Cdc42 regulates filopodium formation (23, 35, 42, 43). In addition, these three proteins can act in a hierarchical cascade, where Cdc42 activates Rac, which in turn activates Rho (35, 43). Many extracellular stimuli induce actin reorganization via Rho family proteins. Lysophosphatidic acid induces the formation of actin stress fibers in quiescent Swiss 3T3 fibroblasts, a response that is dependent on Rho (42). Growth factors such as insulin, platelet-derived growth factor, and bombesin stimulate the polymerization of actin to form lamellipodia and membrane ruffles (43). Bradykinin induces Cdc42-mediated filopodium formation and the subsequent formation of lamellipodia (23). Rho is also required for the formation of focal adhesions, where stress fibers are connected to the extracellular matrix via clustered transmembrane integrins, whereas Rac and Cdc42 regulate the formation of smaller focal complexes, which are similar to focal adhesions in composition but are associated with lamellipodia and filopodia (35).

Many targets of Rho family GTPases have been characterized recently, although the molecular mechanism underlying their ability to regulate actin organization appears complex and still remains unclear. However, the characterization of proteins that bind Rho in a GTP-dependent manner has provided major insights into Rho-mediated signalling. The serine/threonine kinase ROKα/Rho kinase and its close relative p160ROCK/ROKβ play a role in the formation of stress fibers and focal adhesions (20, 26, 27, 33). A model in which Rho kinase induces the interaction of myosin with actin filaments by stimulating the phosphorylation of the myosin light chain (MLC) has been proposed (12). Rho kinase leads to a decrease in MLC phosphatase activity (22) and, more recently, it has been shown that Rho kinase stoichiometrically phosphorylates MLC at the same site that is phosphorylated by MLC kinase (3). This model may underlie the involvement of Rho in regulating cytokinesis, motility, and smooth muscle contraction (52). It has also been suggested that the effect of Rho on MLC

* Corresponding author. Mailing address: The Ludwig Institute for Cancer Research, 91 Riding House St., London W1P 8BT, United Kingdom. Phone: (44)-171-878-4088. Fax: (44)-171-878-4040. E-mail: anne@ludwig.ucl.ac.uk.

leads to stress fiber formation, generating tension that then induces the aggregation of integrins. This process in turn stimulates the formation of focal adhesions and tyrosine phosphorylation of focal adhesion proteins (9). However, other studies have suggested that stress fiber assembly and focal adhesion formation can be regulated independently; for example, Rho and Rho kinase can induce some formation of focal adhesions under conditions in which actin stress fibers are disrupted (11, 35).

Actin reorganization is mediated by Rho family proteins, but the specific response regulated by each protein is highly cell type dependent. In MDCK epithelial cells, lamellipodium formation requires Rac, but Rac is not sufficient by itself to induce lamellipodia when microinjected into the cells (41). Instead, Rac actually enhances the formation of intercellular junctions (50). In neuronal cells, which do not have stress fibers, several factors induce cell rounding and neurite retraction in a Rho-dependent manner (21, 38). In an epidermoid carcinoma cell line, Rac and Rho each regulate a distinct type of ruffling response (34).

Because of these differences, we have extensively characterized the roles of Rho family proteins in MDCK epithelial cells and Bac1.2F5 macrophages (2, 41), two cell types with very different phenotypes. MDCK cells have stress fibers associated with integrin-containing adhesion complexes (14, 41). Hepatocyte growth factor/scatter factor (HGF/SF) stimulates the motility of epithelial cells, inducing centrifugal spreading of cell colonies, disrupting junctions between cells and, consequently, producing cell scattering. Simultaneously, changes in the actin cytoskeleton, including an overall decrease in the amount of stress fibers, the disappearance of peripheral actin bundles at the edges of colonies, and an increase in lamellipodium extension and membrane ruffling, are observed. These changes involve Ras, Rac, and Rho proteins (41). Bac1.2F5 macrophages do not have stress fibers or the associated focal adhesions found in other cultured cells. They are dependent on colony-stimulating factor 1 (CSF-1) for both proliferation and viability, even in the presence of fetal calf serum (5). Bac1 cells become rounded in the absence of CSF-1, and on readdition, the cells rapidly spread, producing filopodia, membrane ruffles, and lamellipodia (2, 5). Rac and Cdc42 are activated in parallel by CSF-1, inducing the formation of lamellipodia and ruffles and of filopodia, respectively, and Rac subsequently activates Rho to stimulate the formation of actin cables within the cell body. CSF-1 also induces the redistribution of focal complexes, and this process is controlled by Cdc42 acting upstream of Rac (2).

Although Rho family proteins have been implicated in many different cell events, the molecular mechanisms underlying these responses have not been fully elucidated, and the identification of additional proteins that interact with them will help to unravel these signalling pathways. We have cloned the mouse *RhoE* gene and studied the biochemical and biological properties of its product. RhoE is able to bind and hydrolyze GTP, although the rate of hydrolysis is much slower than that of other Rho family proteins. Distinct types of actin reorganization were observed when this protein was microinjected into MDCK epithelial cells and Bac1.2F5 macrophages. Specifically, a complete disappearance of stress fibers was observed in MDCK cells, while actin-rich extensions resembling filopodia and pseudopodia were revealed in Bac1.2F5 macrophages. In addition, RhoE was able to increase the speed of migration of HGF/SF-stimulated MDCK cells.

MATERIALS AND METHODS

Screening protocol and cDNA cloning. A Rho-related clone was identified as a PCR product in experiments aimed at cloning human cDNAs from monochromosomal hybrids. Southern analysis demonstrated that the clone was of murine origin and was an example of mispriming. The clone was used to screen an 8.5-day-postcoitum (dpc) whole-mouse-embryo cDNA library. Four tertiary positive clones (r13, r15, r16, and r20) were obtained after a screen of 5×10^5 plaques. Subcloning into pBluescript and sequencing showed that these clones encoded an incomplete open reading frame (ORF) related to RhoA. To obtain a cDNA encoding the full-length protein, the r13 clone was ^{32}P labelled by random priming (multiprime DNA labelling system; Amersham) and used as a hybridization probe to screen a 10-dpc mouse embryo cDNA library under high-stringency screening conditions. Of 2×10^6 plaques screened, 17 positive clones were isolated in the primary screening. Two clones were selected on the basis of their strong hybridization to a probe from the 5′ region of r13, subcloned into pBluescript, and sequenced by dye terminator cycle sequencing with AmpliTaq DNA polymerase (Perkin-Elmer).

Expression and purification of the recombinant protein. Mouse RhoE cDNA generated by PCR was fused to the carboxy-terminal end of the glutathione *S*-transferase (GST) gene by cloning into the *Bam*HI/*Eco*RI sites of the pGEX-2T vector (47). The following primers were used: 5′CGGGATCCGATC CTAATCAG3′ and 5′CGGAATTCTCACATCACAGTACAG3′. RhoE was purified by binding to glutathione beads (Pharmacia Biotech) and cleaved with thrombin to remove GST as previously described (43) but with modification. RhoE was purified from protease-deficient *Escherichia coli* BL21, as protein degradation was observed in strain JM101. In BL21, protein expression was induced by 1 h of incubation with isopropyl-β-D-galactopyranoside (IPTG) at 24°C. Under these conditions, RhoE migrated at an approximate size of 29 kDa on sodium dodecyl sulfate-polyacrylamide gel electrophoresis, whereas with JM101, the size was about 25 kDa. The correct size of the purified protein was confirmed by laser desorption mass spectrometry. For expression in mammalian cells, RhoE cDNA was tagged at the 5′ end by PCR with a DNA sequence encoding the epitope from Myc recognized by the 9E10 antibody and subcloned into the eukaryotic expression vector pEXV-3 (43). The primers used were 5′CGGAATTCCACCATGGAGCAGAAGCTGATCTCCGAGGAGGACCT GGATCCTAATCAGC3′ and 5′CGGAATTCTCACATCACAGTACAG3′. All sequences were checked by dye terminator cycle sequencing with AmpliTaq DNA polymerase.

Guanine nucleotide-binding assay. The active protein concentration was determined by a guanine nucleotide nitrocellulose filter-binding assay (46). Different amounts of RhoE (2 to 25 μg) were incubated in a total volume of 40 μl of assay buffer (50 mM Tris-HCl [pH 7.5], 1 mM dithiothreitol [DTT]) containing 5 mM EDTA and 0.2 μl of [^{3}H]GTP (1 mCi/ml, 8 Ci/mmol; Amersham) or [^{3}H]GDP (1 mCi/ml, 13 Ci/mmol; Amersham) for 30 min at 37°C. Samples were diluted with 1 ml of ice-cold wash buffer containing 50 mM Tris-HCl (pH 7.5), 5 mM $MgCl_2$, and 50 mM NaCl and filtered through prewetted nitrocellulose filters. Before the filters dried, they were washed with 10 ml of cold wash buffer. Radioactivity bound to RhoE was determined by scintillation counting. The active protein concentration was calculated as previously described (46), except that if 1 mol of RhoE binds 1 mol of [^{3}H]GTP, then 1 μg of RhoE should yield approximately 3×10^5 dpm. The total protein concentration was estimated with a protein assay kit (Bio-Rad).

GTPase assay. RhoE (150 ng) was preloaded with [γ-^{32}P]GTP (6,000 Ci/mmol, 10 mCi/ml; DuPont NEN) in 20 μl of 20 mM Tris-HCl (pH 7.5)–25 mM NaCl–0.1 mM DTT–0.5 mg of bovine serum albumin (BSA) per ml–4 mM EDTA for 30 min at 37°C. $MgCl_2$ was added at a final concentration of 20 mM on ice. Eighteen nanograms of the preloaded protein was diluted into 20 mM Tris-HCl (pH 7.5)–0.1 mM DTT–1 mg of BSA per ml–1 mM GTP to give a final volume of 30 μl. Aliquots (5 μl) were removed after incubation for 0, 5, 10, 15, and 30 min and for 1 h at 37°C and diluted with an ice-cold buffer (50 mM Tris-HCl [pH 7.5], 50 mM NaCl, 5 mM $MgCl_2$). Radioactivity bound to RhoE was measured by scintillation counting.

Cell culture and microinjection. MDCK cells were incubated at 37°C (10% CO_2) in Dulbecco's modified Eagle's medium (DMEM) containing 10% bovine fetal calf serum (FCS). For microinjection, cells were seeded at 5×10^3 per well (15-mm diameter) on glass coverslips (13 mm) marked with a cross to facilitate the localization of injected cells. After 3 days, cells were transferred to DMEM containing 5% FCS. For analysis of actin organization, approximately 50% of the cells in a colony were microinjected. RhoE was injected at 40 to 50 μg/ml (determined by [^{3}H]GTP binding), and V14RhoA (constitutively active RhoA [amino acid 14 altered from Gly to Val] [42]) was injected at 200 μg/ml (determined by [^{3}H]GDP binding). To identify injected cells, rat immunoglobulin G (IgG) or rabbit IgG (Pierce) at 0.5 mg/ml was microinjected together with the recombinant protein. Proteins were diluted in 50 mM Tris-Cl (pH 7.5)–100 mM NaCl–5 mM $MgCl_2$. The pEXV-3 expression plasmid carrying Myc-tagged *RhoE* cDNA was injected at 0.3 mg/ml in phosphate-buffered saline (PBS; Gibco BRL).

A subclone of the cloned mouse macrophage line Bac1.2F5 (32) was grown at 37°C (10% CO_2) in T25 tissue culture flasks (Falcon). Except as stated otherwise, all media and supplements used with macrophages were supplied by ICN Flow. Cells were maintained in DMEM supplemented with 10% heat-inactivated FCS

(Biopharm UK), 1.32 nM CSF-1 (Chiron Corp.), 2 mM L-glutamine, 0.15 mM L-asparagine, 15 nM β-mercaptoethanol, 77.5 U of streptomycin per ml, and 25 U of penicillin per ml. Cells were subcultured twice weekly by dissociation with 0.04% EDTA in PBS and resuspended in growth medium at 2×10^5 cells/ml. For microinjection, 5×10^4 cells per well were plated in wells containing 13-mm glass coverslips and microinjected 48 h after seeding.

The R4.2 cell line is a clone derived from the HB4a mammary luminal epithelial cell line (36) by transfection with oncogenic H-Ras cDNA; it was a gift from Robert Harris and Thomas Eichholtz (GlaxoWellcome, Stevenage, United Kingdom). R4.2 cells were grown at 37°C (5% CO_2) in RPMI 1640 with L-glutamine, 10% FCS, and insulin (5 μg/ml). Cells were seeded at 10^4 per well on glass coverslips and microinjected 2 days later.

Immunofluorescence. For immunofluorescence analysis, cells were washed briefly in PBS containing 0.9 mM $CaCl_2$ and 0.7 mM $MgCl_2$ and then fixed for 20 min in 3.7% formaldehyde in PBS at room temperature. Cells were permeabilized with 0.2% Triton X-100 in PBS for 5 min. Actin filaments were localized by incubating cells for 45 min with 0.1 μg of tetramethyl rhodamine isothiocyanate (TRITC)-labelled phalloidin (Sigma Chemical Co.) per ml as previously described (42). Cells containing rat IgG or rabbit IgG (microinjection marker) were localized with fluorescein isothiocyanate (FITC)-conjugated goat anti-rat IgG (1:400; Sigma) or FITC-conjugated goat anti-rabbit IgG (1:200; Southern Biotechnology Associates, Inc.). For localization of cells expressing the tagged RhoE cDNA, fixed cells were blocked for 1 h in PBS containing 10% FCS, 5% milk powder, 0.5% BSA, and 0.1% Triton X-100. They were then incubated with an anti-Myc mouse monoclonal antibody, 9E10 (1:400; Santa Cruz Biotechnology), in 1% BSA, followed by incubation with FITC-conjugated goat anti-mouse IgG (1:400; Jackson ImmunoResearch) in 1% BSA together with TRITC-conjugated phalloidin.

Confocal laser scanning microscopy. Images of cells were visualized with an MRC 500 confocal visualization system (Bio-Rad) or with an LSM 310 apparatus (Zeiss, Welwyn Garden City, United Kingdom) mounted over an infinity-corrected Axioplan microscope by using a ×10 eyepiece and a ×63 NA 1.4 oil immersion objective (Zeiss). The MRC 500 was configured and used as described previously (15). Image files were collected with the LSM 310 as a matrix of 1,024 by 1,024 pixels describing the average of eight frames scanned at 0.062 Hz, where FITC and TRITC were excited at 488 nm and 543 nm and visualized with bandpass filters of 540 ± 25 and 608 ± 32 nm, respectively, where the levels of interchannel cross talk were insignificant. Three-dimensional data sets were obtained with the MRC 500 by collecting a series of single views as the stage was moved 0.37 μm along the *z* axis between each view.

Time-lapse videomicroscopy. MDCK colonies chosen for each experiment contained 15 to 20 cells, and every cell in each colony was microinjected. Some of the colonies were microinjected with RhoE, and others were microinjected with a control protein, usually rabbit IgG. For experiments studying the motility of MDCK cells, recombinant human HGF/SF (R&D Systems) was added after microinjection at a final concentration of 5 ng/ml. Cells were filmed on a Zeiss ICM 405 microscope linked to a Panasonic F15 camera and a Hamamatsu image processor with a Sony U-matic time-lapse video recorder.

RESULTS

Isolation and analysis of a mouse cDNA that codes for a Rho-related protein. Partial cDNAs encoding part of a novel Rho family protein were originally isolated in a screen for novel human cDNAs (see Materials and Methods). A cDNA encoding the full-length ORF was subsequently isolated from a 10-dpc mouse embryo library. The identified ORF extends over 690 bp and encodes a protein of 229 amino acids.

Alignment of this sequence to other members of the Rho family demonstrated that the nucleotide sequence is 92% identical to human *RhoE* cDNA and 100% identical at the amino acid level to the RhoE protein recently described by Foster et al. (16). Phylogenetic analysis of the mouse RhoE protein showed that it is more homologous to the Rho subfamily than to the Rac and Cdc42 subfamilies (Fig. 1). This finding is also corroborated by the fact that its effector domain (amino acids 32 to 42) is more closely related to RhoA, RhoB, and RhoC than to Rac or Cdc42. It is most closely related to human Rho6, Rho7, and Rho8, proteins whose sequences have not yet been published but are available in the EMBL database.

The predicted size of mouse RhoE is approximately 25.6 kDa, as determined from its sequence. The RhoE gene is expressed as a 3.3-kb mRNA detected in different rodent cell lines, including Rat-2, NIH 3T3, and Swiss 3T3 fibroblasts and Bac1.2F5 macrophages (data not shown).

Biochemical characterization of the mouse RhoE protein. Since the activity of Rho-related GTPases is regulated by their ability to bind and exchange guanine nucleotides and to hydrolyze GTP, we tested whether RhoE behaved in a manner similar to that of other Rho family members. RhoE was expressed as a GST fusion protein in *E. coli*, the GST was removed with thrombin, and the purity of the cleaved RhoE was confirmed by sodium dodecyl sulfate-polyacrylamide gel electrophoresis and Coomassie blue staining. The correct size was confirmed by laser desorption mass spectrometry. A nucleotide-binding assay where [^{3}H]GTP was incubated with RhoE showed that this protein is capable of binding GTP (Fig. 2A) and demonstrated a linear relationship between GTP bound and increasing concentrations of RhoE. In addition, the amount of GTP bound to a constant concentration of RhoE increased as the GTP concentration was increased, reaching a maximum value at 6 μM GTP (data not shown). In contrast to [^{3}H]GTP, RhoE (25 μg/ml) did not detectably bind [^{3}H]GDP after 10 min of incubation (Fig. 2B) or when different RhoE concentrations, [^{3}H]GDP concentrations, and incubation times were tested (data not shown).

The intrinsic GTPase activity of RhoE was also studied, showing that under conditions where Rac hydrolyzes 95% of [γ-^{32}P]GTP, RhoE hydrolyzed approximately 31% (Fig. 2C). The curve is biphasic, with a higher initial rate of GTP hydrolysis during the first 10 min followed by much lower GTPase activity. RhoE thus exhibits GTPase activity, but the hydrolysis rate is very low compared to that of other Rho family proteins. The uncleaved GST-RhoE fusion protein also hydrolyzed GTP (data not shown). To confirm that the reduction in radioactive nucleotide remaining on RhoE was in fact due to the hydrolysis of the phosphate group itself and not to spontaneous exchange, we performed the same hydrolysis assay with [^{3}H]GTP (more than 95% of the radioactivity is associated with the guanine moiety). No decrease in [^{3}H]GTP binding to RhoE was detected during a 30-min incubation (data not shown), ruling out the possibility that the GTP molecule was released rather than hydrolyzed.

RhoE induces stress fiber disassembly in MDCK cells. Rho family proteins are known to be involved in regulating actin organization, although the precise response varies between cell types (52). We therefore investigated responses to RhoE in two different cell types, MDCK epithelial cells and Bac1.2F5 macrophages, for which we have previously characterized responses to other Rho family proteins (2, 41). Our initial aim was to determine whether RhoE had any effect on cytoskeletal reorganization, which plays a crucial role in many cellular processes, including motility, cytokinesis, and phagocytosis.

MDCK is an epithelial cell line that proliferates as discrete colonies and becomes motile in response to HGF/SF (48). It is believed that changes in actin polymerization and depolymerization are involved in driving cell motility (13). Purified RhoE was microinjected into unstimulated colonies containing 40 to 50 cells (3 days after plating), and its effect on the actin cytoskeleton was investigated by confocal microscopy. Unstimulated MDCK cells have actin stress fibers localized close to the basal membrane. RhoE induced the total disappearance of stress fibers when microinjected into both cells at the periphery of (Fig. 3A and B) and cells within (Fig. 3C and D) colonies. Many of the injected cells had aggregates of actin filaments within the cytoplasm. These changes in the actin cytoskeleton induced by RhoE were rapid and were observed by 10 min after microinjection, at concentrations of active RhoE protein of >15 μg/ml. The effect of RhoE diminished with time, and at 10 h after RhoE microinjection, most injected cells had fine actin filaments, mainly at the cell periphery, and actin aggre-

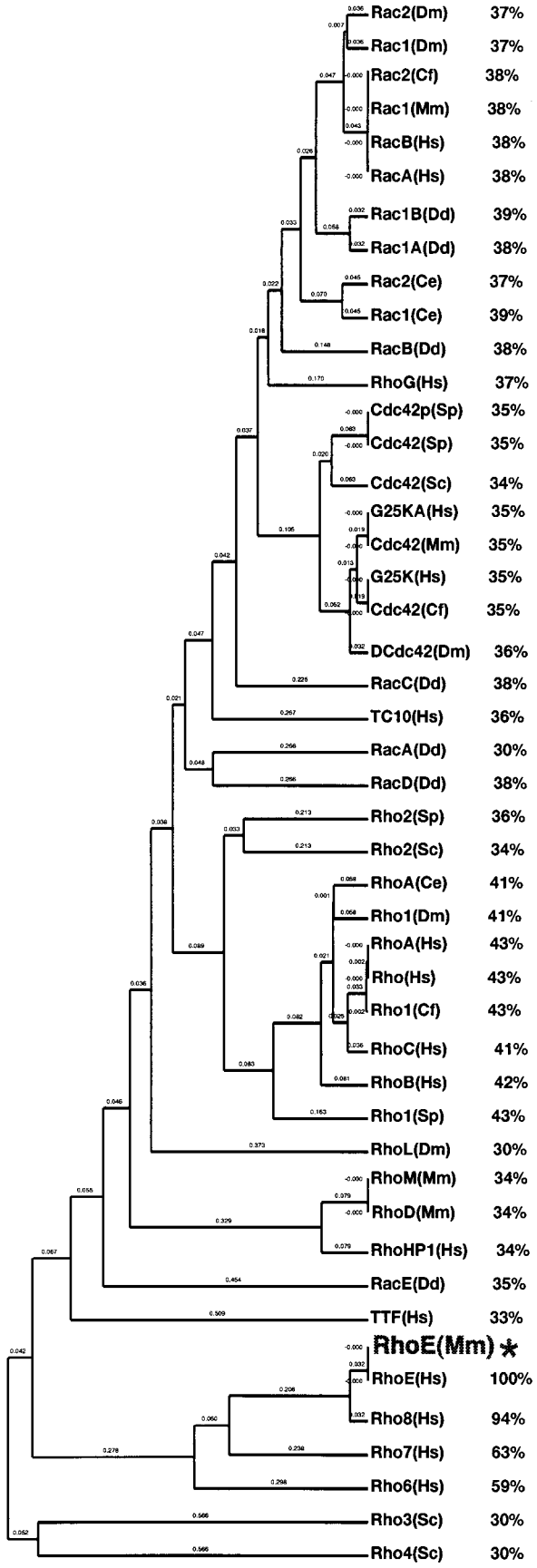

gates were not present (data not shown). These results suggested that by 10 h the cells were reverting to their original actin cytoskeleton phenotype. RhoE also induce a dramatic decrease in the number of focal adhesions, as determined by staining for vinculin (data not shown). Since RhoE affects stress fibers, which are known to be induced by RhoA (42), we wondered whether RhoE could inhibit the response to RhoA. Microinjection of both V14RhoA (50 μg/ml) and RhoE (25 μg/ml) together led to an increase in the amount of stress fibers similar to that observed with V14RhoA alone (data not shown), suggesting that RhoA is able to overcome the RhoE effect in MDCK cells.

MDCK cells also exhibit bundles of actin fibers running parallel to the outer membranes of many cells at the basal edges of colonies. Approximately 15% of outer cells do not have these bundles of actin fibers and instead extend lamellipodia from the smooth outer edges of colonies (41). These peripheral actin bundles, as well as stress fibers, disassemble in cells injected with C3 transferase, which inhibits Rho (41). In contrast, RhoE did not detectably alter these structures when microinjected into cells at the periphery of colonies, even up to 10 h after microinjection (shown at 30 min in Fig. 3A and B). Even at the highest concentration of RhoE attainable when purified from *E. coli* (65 μg of active protein per ml), no effect on peripheral actin bundles was observed (data not shown). RhoE also did not obviously affect lamellipodium formation (Fig. 3A and B). To confirm that the observed changes in actin organization were not due to the microinjection protocol itself, we microinjected IgG into MDCK cells. Stress fibers, as well as actin bundles at the periphery of colonies, were retained in these control injected cells (Fig. 3E and F).

To verify that the cytoskeletal reorganization was indeed due to the RhoE protein itself, we microinjected a eukaryotic expression vector containing myc epitope-tagged *RhoE* cDNA into the nuclei of MDCK cells. Four to six hours after injection, stress fiber loss was observed together with aggregates of actin filaments (Fig. 4B). These experiments also allowed the subcellular localization of RhoE to be analyzed. As revealed by immunofluorescence with an anti-myc epitope antibody, RhoE was localized throughout the cytoplasm but was also strongly associated with the plasma membrane (Fig. 4A). In addition, it colocalized with the aggregates of actin filaments which were induced by RhoE expression (Fig. 4B). A series of *z* sections through the cells obtained by confocal microscopy showed that these aggregates were present on the basal surfaces of cells (Fig. 4C), suggesting a link with stress fiber disruption, and were not present on the apical surfaces (Fig. 4D). RhoE was associated with the plasma membrane on the lateral membrane between cells, mainly between the middle of the cells and the apical surface, as well as on the apical membrane in structures that resembled microvilli (Fig. 4D). Indeed, analysis of a series of *z* sections showed that these structures had a distribution and an appearance similar to those of microvilli, as revealed in cells stained for actin filaments (data not shown).

Actin reorganization in Bac1.2F5 macrophages induced by RhoE. Bac1.2F5 macrophages are a hemopoietic cell line

FIG. 1. Phylogenetic analysis of Rho family proteins, including percentages of homology between mouse RhoE (asterisk) and the other proteins. Mouse *RhoE* cDNA was identified by screening of a 10-dpc mouse embryo library. It shares the five conserved GTP-binding domains that are found in all other Ras-related proteins and are known to be important for their function. It exhibits very strong sequence similarity to Rho6, Rho7, and Rho8. Sequences were aligned with the Geneworks program by use of the Clustal algorithm and a PAM250 table.

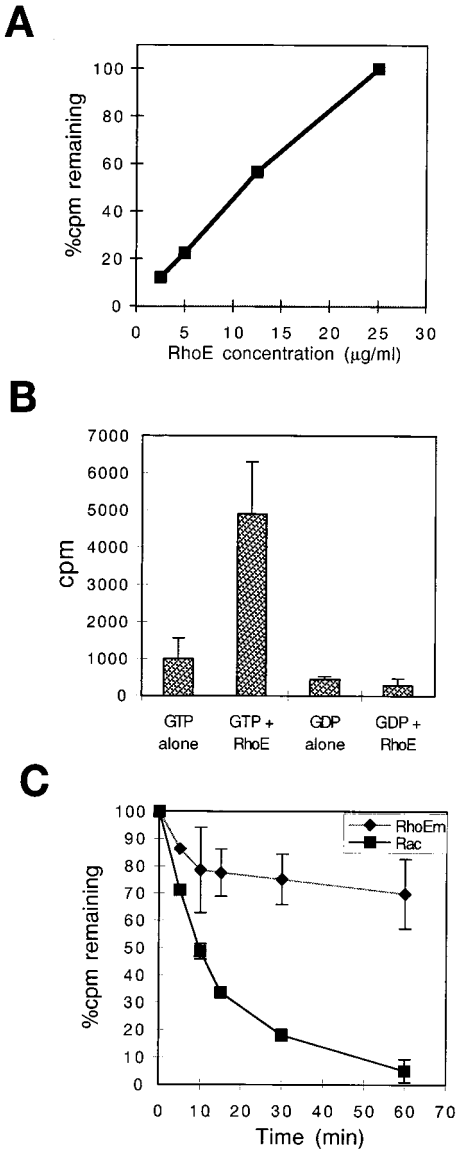

FIG. 2. RhoE binds and hydrolyzes GTP, but the intrinsic GTPase activity is low compared to that of other Rho proteins. (A) GTP-binding assay. Recombinant RhoE was expressed as a GST fusion protein in a protease-deficient strain (BL21), bound to glutathione-agarose beads, and cleaved with thrombin. RhoE at the indicated concentrations was incubated at 37°C with [^{3}H]GTP for 30 min, and radioactivity bound to the protein was determined by a filter-binding assay. (B) Comparison of GTP and GDP binding. A nucleotide-binding assay with [^{3}H]GDP showed background levels of radioactivity when GDP was incubated with RhoE at 25 μg/ml. (C) Intrinsic GTPase activity of thrombin-cleaved RhoE and Rac. Each protein was preloaded with [γ-^{32}P]GTP, incubated at 37°C in the presence of excess unlabeled GTP for the indicated times, and subjected to a filter-binding assay. The amount of radioactivity remaining bound to each protein was determined by scintillation counting. RhoEm, mouse RhoE.

whose actin cytoskeletal organization is different from that of epithelial cells. They do not possess stress fibers or the focal adhesions found in many other cultured cell types. Instead, they exhibit an actin cytoskeleton organized as very fine actin cables within the cytoplasm, regulated by RhoA and thought to be the counterpart of the stress fibers in other cell types (2). They depend on CSF-1 for both viability and proliferation. Bac1.2F5 cells became rounded in the absence of CSF-1 (Fig. 5B), and on readdition they spread, adopting the typical phenotype of growing cells (Fig. 5A). To investigate if RhoE had any effect on the actin cytoskeleton, RhoE protein was microinjected into these cells. After 10 min, this protein rapidly induced a reorganization in actin distribution, leading to a striking difference in cell morphology. Cells extended long actin-rich extensions resembling filopodia and pseudopodia (Fig. 5C and D). Time-lapse videomicroscopy confirmed that these structures were actively extended from cells following the microinjection of RhoE (data not shown). A more detailed study revealed that these structures appeared in two slightly different phenotypes, some with broad, web-like actin-containing structures linking filopodium-like structures (Fig. 5C) and others with smaller pseudopodia among longer and more numerous filopodium-like structures (Fig. 5D). These different formations may reflect both the intrinsic morphological heterogeneity of these macrophages and the different patterns of actin organization that they exhibit, as was previously postulated with monocytes (1). Microinjection of a control protein (IgG) did not induce any change in Bac1.2F5 morphology, confirming that the responses to RhoE were not due to microinjection itself (Fig. 5E and F).

Similar morphological changes were obtained when the expression vector carrying myc epitope-tagged *RhoE* cDNA was microinjected into the nuclei of Bac1.2F5 macrophages and the expressed RhoE protein was detected with antibody 9E10 against the myc epitope (Fig. 5G). The cellular distribution of RhoE was also revealed by these immunofluorescence studies. RhoE was expressed throughout the cytoplasm but strongly localized at the dorsal plane of Bac1.2F5 macrophages, specifically at the level of the ruffles, as revealed by three-dimensional reconstruction of a series of *z* sections obtained by confocal microscopy (Fig. 5H).

Stimulation of cell migration speed by RhoE. MDCK cells become motile in the presence of HGF/SF, and this response involves initial centrifugal spreading of cells followed by detachment of cells from each other (scattering) (48). It has been reported that HGF/SF induces actin cytoskeletal reorganization, including a decrease in the amount of stress fibers and the extension of lamellipodia, both of which are likely to be important for the migration response (13, 14, 41). It has also been shown that the microinjection of V14RhoA induces stress fiber formation and inhibits HGF/SF-induced motility (41). Since RhoE alters actin organization in MDCK cells, it is possible that this protein has an effect on motility.

The effect of RhoE on the responses to HGF/SF was investigated by monitoring cell motility by time-lapse videomicroscopy. At RhoE concentrations of 25 μg/ml, MDCK cells were able to spread and scatter. During the first 4 to 6 h after the addition of HGF/SF, the surface area of each epithelial cell and therefore of each colony increases, with the subsequent scattering response involving the breaking of contact among cells. To study cell locomotion specifically associated with scattering and not spreading, cells were tracked from 5 to 15 h after the addition of HGF/SF. Figure 6 shows that the migration speed of MDCK cells was significantly increased by 30% with RhoE injection, as revealed by a statistical Student *t* test ($P \leq 0.001$), compared to the speed of control cells injected with rabbit IgG.

To confirm that the effect of RhoE on MDCK cell migration was not specific for one cell line, we also studied the motility of another cell line, a human mammary luminal epithelial cell line, R4.2, which expresses activated Ha-Ras (see Materials and Methods). This cell line does not proliferate in colonies, and the growing cells are normally motile (Fig. 6). Microinjection of RhoE induced a significant increase of 37% ($P \leq 0.04$) in the migration speed of R4.2 cells compared to the speed of

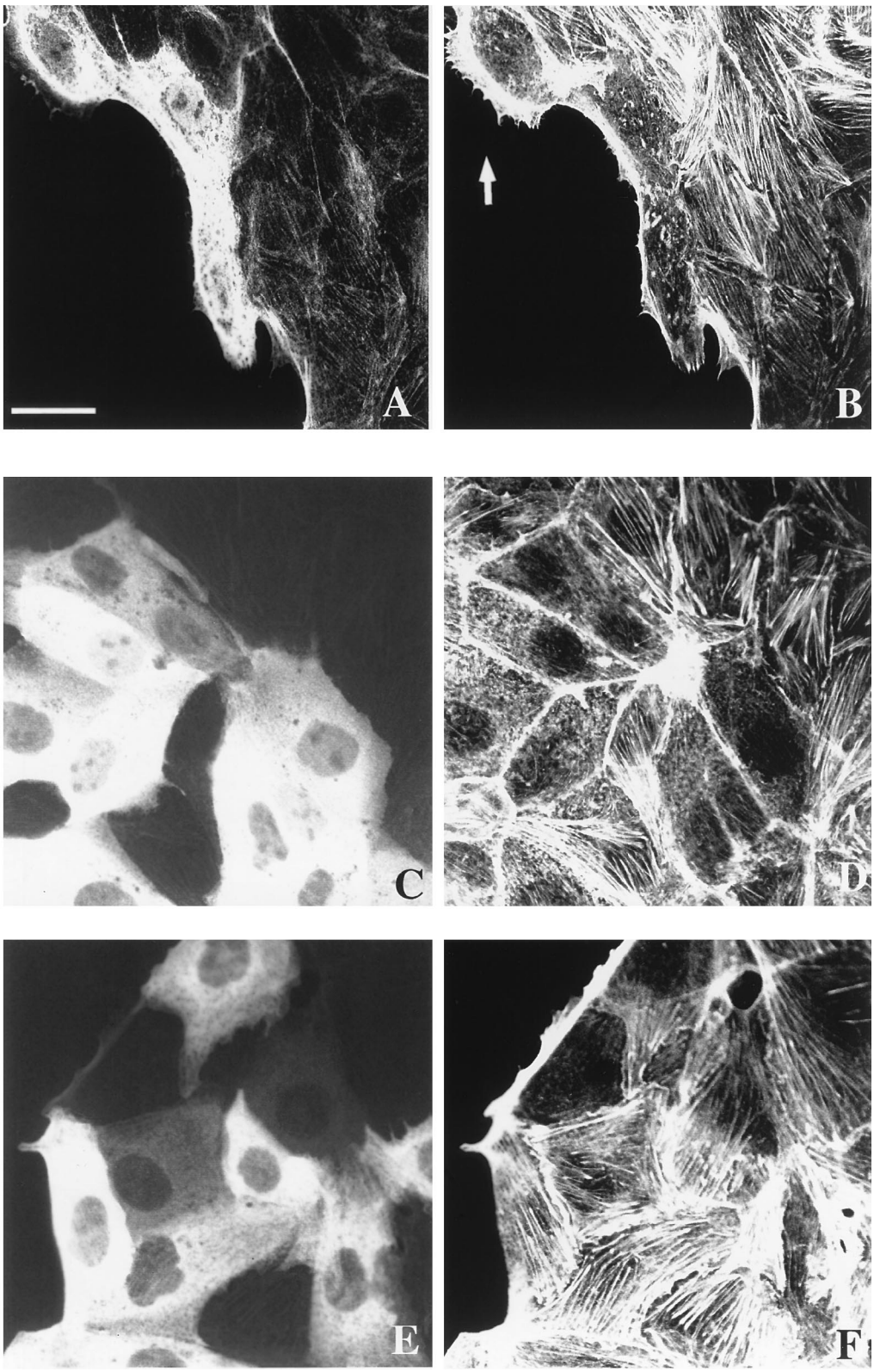

FIG. 3. RhoE induces the disappearance of stress fibers in MDCK cells. Confocal micrographs of cells injected with recombinant RhoE at 25 μg/ml and rat IgG (0.5 mg/ml) (A, B, C, and D) or rat IgG alone at 0.5 mg/ml (E and F) (as a marker to identify injected cells) are shown. Actin filaments were localized (B, D, and F) by staining with TRITC-labelled phalloidin 30 min after RhoE injection at both the periphery (B) and within a cell colony (D) or after injection with IgG alone (F). Microinjected cells were detected with FITC-labelled goat anti-rat IgG (A, C, and E). Arrow in panel B, RhoE-injected cell with a lamellipodium. The scale bar represents 42 μm (A and B) or 25 μm (C, D, E, and F).

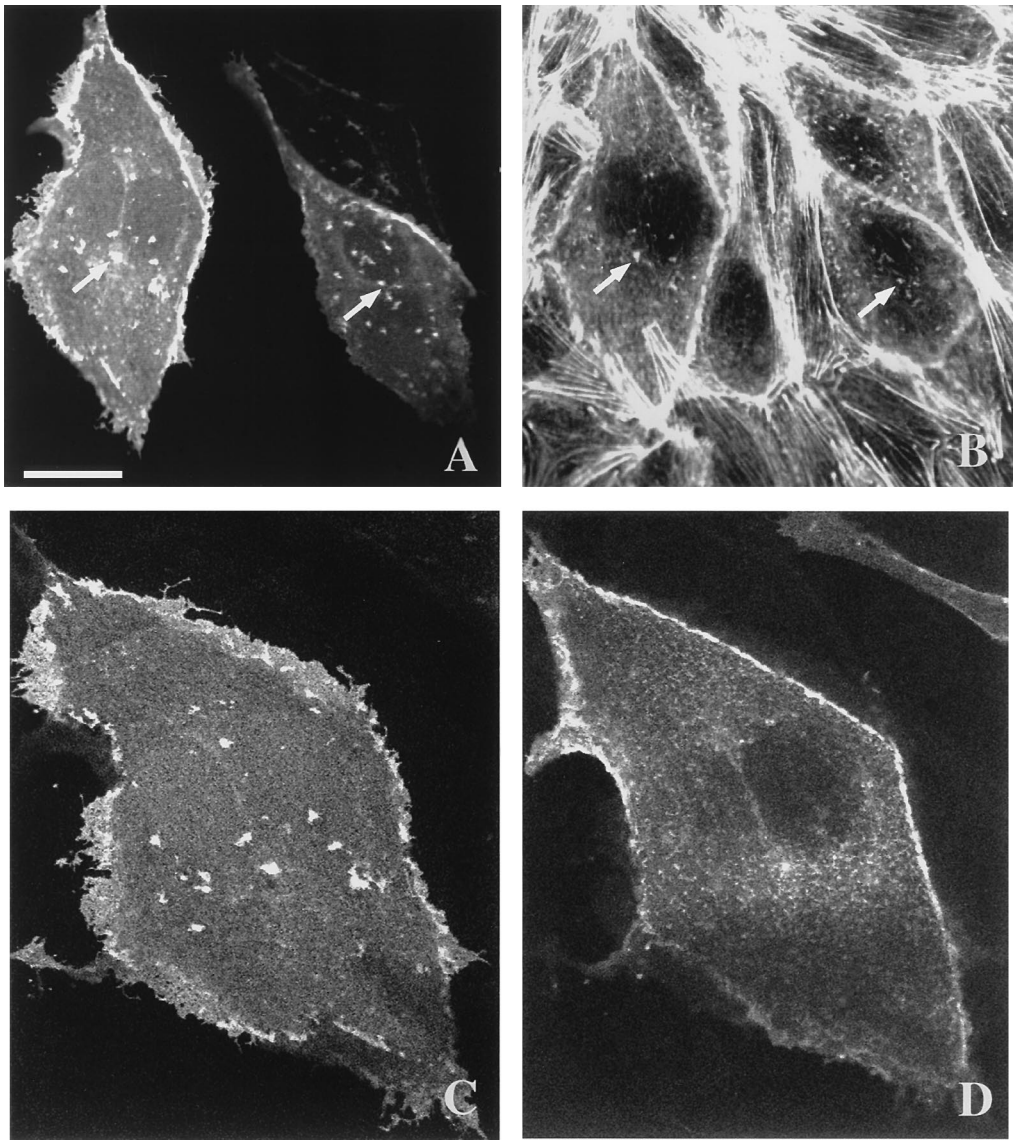

FIG. 4. Immunolocalization of RhoE in MDCK cells. A eukaryotic expression vector, pEXV3, containing myc epitope-tagged *RhoE* cDNA was microinjected into the nuclei of MDCK cells. Cells were analyzed by immunofluorescence to detect myc epitope-tagged RhoE with anti-myc epitope antibody 9E10 followed by incubation with FITC-conjugated goat anti-mouse IgG (A, C, and D) RhoE and TRITC-labelled phalloidin (B) to detect actin filaments. (A and B) Confocal images show that RhoE was localized mainly at the level of the plasma membrane as well as in some structures (arrows) inside the cytoplasm (A) that colocalized with aggregates of actin filaments (B). (C and D) Images show RhoE localization in basal (C) and near-apical (D) optical sections of the left-hand cell in panel A. The scale bar represents 25 μm (A and B) or 15 μm (C and D).

control cells injected with IgG (Fig. 6). Taken together with the RhoE-induced disruption of the actin cytoskeleton, these results suggest that the disappearance of stress fibers and focal adhesions enhances the cell migration rate. This suggestion is in accordance with previous observations in MDCK cells, in which a RhoA-induced dense network of stress fibers antagonizes locomotion (41).

DISCUSSION

The Rho family members Rho, Rac, and Cdc42 are well characterized with regard to regulating the formation of specific actin-containing structures, although the physiological relevance of these responses remains to be established. In addition, the functions of most other members of the family are unclear. We have cloned the mouse homolog of the human *RhoE* gene (16) and investigated its role in regulating actin organization. Phylogenetic studies show that RhoE is more closely related to RhoA, RhoB, and RhoC than to Rac and Cdc42 and, interestingly, this protein has the same effector domain as RhoA, RhoB, and RhoC (16), except for amino acid 36 (Asn), analogous to position 31 in Ras (Val) (Fig. 7). This domain is important in Ras superfamily proteins for interactions with downstream targets. In contrast, in the region corresponding to the insert helix of RhoA and Rac1 (residues 124 to 136 in RhoA), a structure exclusive to Rho family proteins (19, 53), only 5 of 13 amino acids are identical between RhoE and RhoA (Fig. 7). RhoE actually shows the strongest sequence similarity to human Rho8, followed by Rho7 and Rho6, for which sequences are available in the EMBL database but are not yet published. These sequences may form a separate subfamily of Rho proteins.

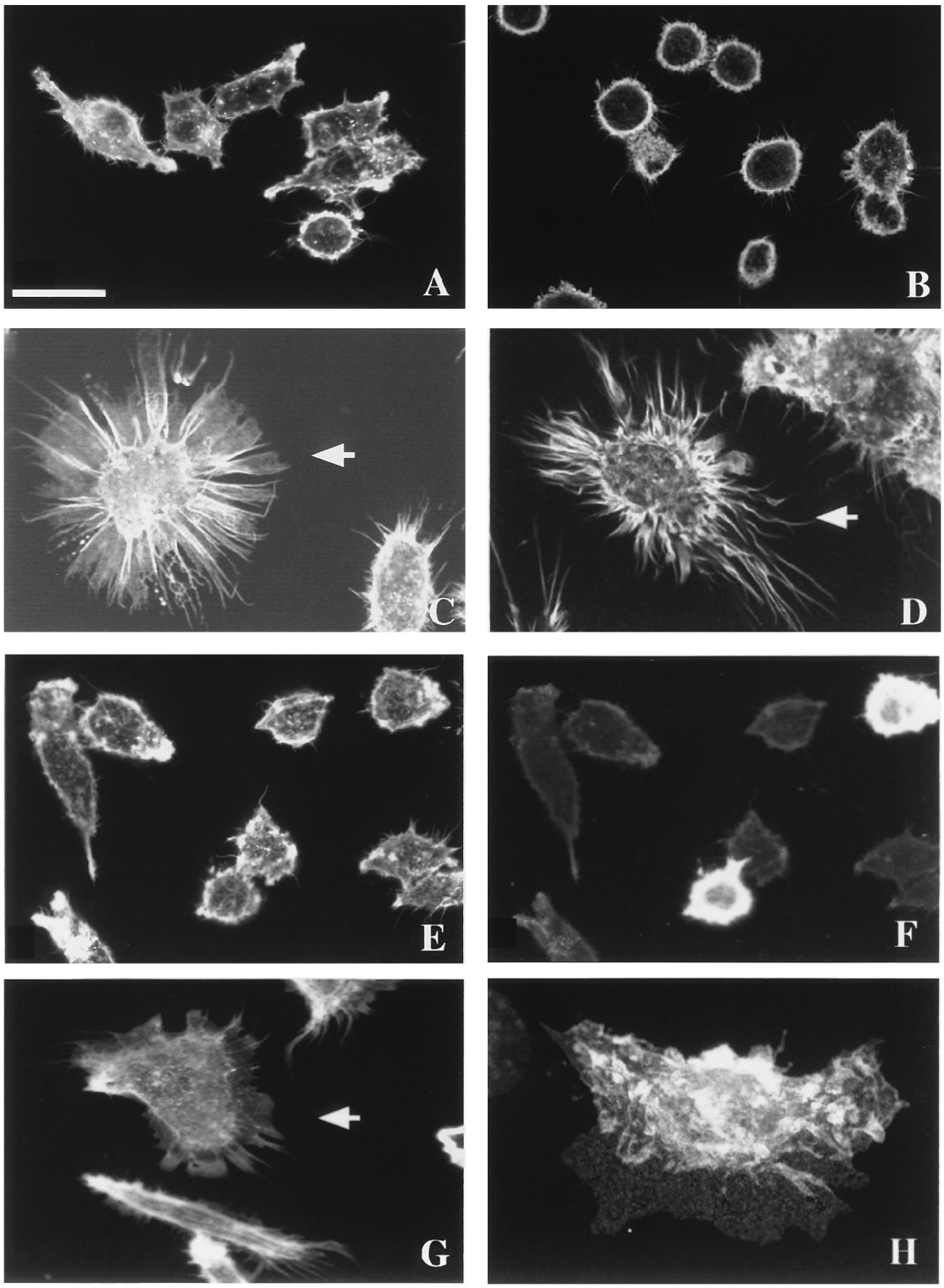

FIG. 5. Actin reorganization induced by RhoE in Bac1.2F5 macrophages. Confocal micrographs show growing (A) and CSF-1-starved (B) cells, cells injected with recombinant RhoE protein at 25 μg/ml (C and D), cells injected with rat IgG at 0.5 mg/ml as a control (E and F), and cells injected with expression vector pEXV3-myc-RhoE at 0.3 mg/ml (G and H). Bac1.2F5 cells were stained with TRITC-labelled phalloidin to reveal actin filaments (A, B, C, D, E, and G), with FITC-labeled goat anti-rabbit IgG (F) to detect microinjected cells, or with anti-myc epitope antibody 9E10 followed by FITC-labeled goat anti-mouse IgG (H). (H) A three-dimensional reconstruction shows the subcellular localization of RhoE 4 h after DNA microinjection. A maximum-intensity projection through a 768- by 512- by 25-voxel data set was generated with the intermediate axis (512 voxels) tilted 15°. Arrows indicate injected cells. The scale bar represents 20 μm (A, C, E, F, and G), 28 μm (B), 17 μm (D), or 14 μm (H).

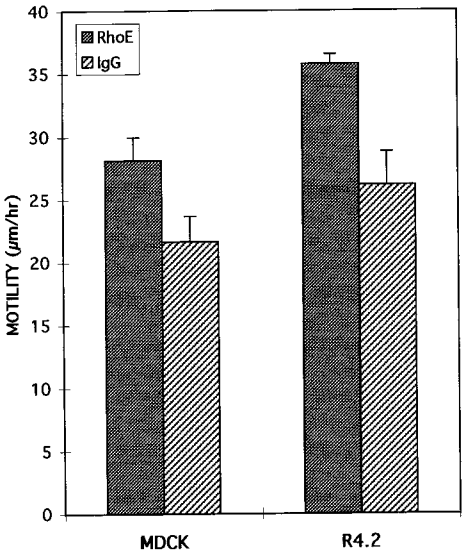

FIG. 6. Enhancement of cell migration speed by RhoE. Cell migration was monitored by tracking injected cells from 5 to 15 h after the injection of RhoE. All cells monitored were microinjected with either RhoE (25 μg/ml) or rabbit IgG (1 mg/ml) as a control protein. HGF/SF (5 ng/ml) was added to MDCK cells 15 min after microinjection, and cells were monitored by time-lapse videomicroscopy. Ten cells were randomly selected, and the positions of their nuclei were tracked every hour. For MDCK cells, five cells at the outer edge and five cells within a colony were tracked. When a cell divided, both progeny were monitored and the mean of the distances that they moved was calculated. The final mean distance migrated was calculated from the average distance moved by each of the 10 cells per hour. The error bars represent the standard deviations of the means (four or five independent experiments for MDCK cells and two for R4.2 cells). The difference in migration rates between RhoE-injected cells and control cells was statistically significant ($P \leq 0.001$ for MDCK and $P \leq 0.04$ for R4.2).

Rho GTPases normally exist in two conformational states, an active GTP-bound form and an inactive GDP-bound form (4). RhoE has the five highly conserved G motifs known to be important for the nucleotide-binding and catalytic functions of the Ras-related protein superfamily (6), and indeed we have found that RhoE efficiently binds GTP, in accordance with previous results obtained with human RhoE (16). However, under our experimental conditions, GDP binding was not detected, suggesting that the affinity for GDP is extremely low and consistent with the observation that RhoE does not bind GDP in vivo (16). RhoE thus appears to differ from other Rho family proteins in not having a stable GDP-bound conformation.

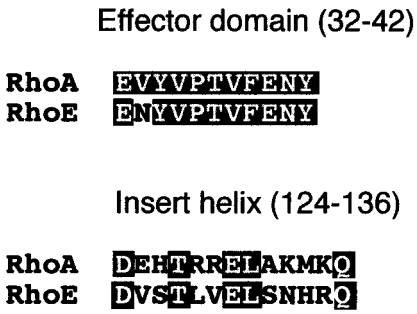

FIG. 7. Comparison of the amino acid sequences of RhoA and RhoE in the effector domain and the insert helix. Sequence alignment between these two proteins showed very similar effector domains (except for one amino acid) but many differences in the insert helices. Letters in white represent identical residues.

RhoE has substitutions at three positions known to be important for GTP hydrolysis (16). It has a serine at each position (17, 64, and 66), equivalent to amino acids 12 (Gly), 59 (Ala), and 61 (Gln) in Ras. Despite these structural differences, we have demonstrated that RhoE exhibits intrinsic GTPase activity (both thrombin-cleaved RhoE and a GST-RhoE fusion), although at a low rate compared with other Rho family proteins. Other GTPases containing substitutions at positions which participate in the binding and hydrolysis of GTP have been reported elsewhere (18, 39). For example, Rap proteins have a threonine instead of the highly conserved glutamine at position 61 (37). Rad and Gem proteins contain substitutions at position 61 (equivalent to position 12 in Ras) in the G1 motif and at position 108 (equivalent to position 60 in Ras) in the strongly conserved DX_2G sequence of the G3 motif (55). However, all of these proteins exhibit GTPase activity. Furthermore, like RhoE, Rad has a low intrinsic GTPase activity, and single mutations at positions equivalent to 12 and 61 in Ras did not affect the Rad GTPase activity, although mutations at both residues increased the GTPase activity (55). Similarly, mutations at the three specific substituted residues in RhoE resulted in an increase in the rate of GTP hydrolysis, observed with the RhoE double mutant A64Q66 and the RhoE triple mutant G17A64Q66 (16). Given the three substitutions in RhoE, it is likely that the mechanism of GTP hydrolysis varies from that defined for Ras. Indeed, it is worth noting that the different structures of GTPases solved so far suggest variations in the exact mechanism of GTP hydrolysis; for example, the crystal structure of RhoA-GDP demonstrates a novel mode of Mg^{2+} binding (53). It is also reasonable to suggest that to turn off RhoE efficiently in vivo, a specific GAP must exist, as has been reported for Rap and Rad (45, 55), although no GAP activity for RhoE was detected in cell extracts (16).

Previous experiments with human RhoE did not detect any GTPase activity (16). The apparent discrepancy between these results and ours may be due to our use of a protease-deficient strain of *E. coli*. We have observed that the RhoE protein from *E. coli* JM101 is slightly truncated, whereas the RhoE protein from a protease-deficient strain, BL21, is full length. Removal of a small portion of the protein could affect the detection of GTPase activity.

As it is known that Rho proteins induce cell-type-specific changes in actin reorganization, we studied the effects of RhoE using two different cell types. MDCK cells have stress fibers associated with integrin-containing adhesion complexes, and microinjection of recombinant V14RhoA stimulates stress fiber formation (41). In contrast, we showed that RhoE microinjection resulted in the rapid disappearance of stress fibers and the appearance of aggregates of actin filaments inside the cytoplasm. These aggregates could well have been the remnants of stress fibers that became detached from focal adhesions, as they disappeared with time after injection. In addition, RhoE induced a loss of focal adhesions, which are also regulated by RhoA (42). Time-lapse videomicroscopy showed that by 10 h after microinjection of RhoE, cells were much flatter and more spread out than control cells (data not shown). Considering that stress fibers act to maintain cell tension, it is likely that the loss of these actin structures directly leads to cell spreading. Indeed, in other cellular systems the loss of stress fibers is accompanied by rapid cell spreading and, interestingly, the overexpression of dominant-negative N-terminally truncated ROKα, a downstream target for RhoA, induces cell spreading in HeLa and Swiss 3T3 cells (26).

Our results suggest that RhoE may inhibit signalling downstream of RhoA to prevent RhoA from stimulating stress fiber formation. One possibility is that it competes with RhoA for

interaction with one or more downstream effectors, explaining our observation that RhoE was unable to inhibit stress fiber formation when coinjected with V14RhoA. This hypothesis is also supported by the fact that RhoA and RhoE have almost identical effector domains (Fig. 7), indicating that they are likely to interact with common downstream targets. However, although RhoE induced the loss of stress fibers, it did not completely mimic the effects of C3 transferase, a specific inhibitor of Rho function (29). MDCK cells have actin bundles at the periphery of colonies which are broken occasionally at places where lamellipodia extend outward (14, 41). Inhibition of RhoA function by C3 transferase microinjection results in the disappearance of these peripheral bundles (41). In contrast, RhoE did not detectably affect the peripheral bundles, at either early or late times after microinjection, even at the highest RhoE concentration we could obtain. It is possible that this result reflects an inability to introduce high enough concentrations of RhoE to inhibit RhoA signalling completely, as peripheral actin bundles are more stable than stress fibers and microinjection of low concentrations of C3 transferase leads to a loss of stress fibers before peripheral actin bundles are disassembled (RMG and AJR, unpublished data). An alternative possibility is that RhoE interacts with some but not all downstream targets of RhoA and that the targets involved in regulating stress fiber formation differ from those involved in peripheral bundle formation. Interestingly, the insert helix (amino acids 124 to 136 in RhoA) is not conserved between RhoA and RhoE (Fig. 7). It has recently been hypothesized that this insert helix may be responsible for conferring effector specificity among Rho family members (53). The effector domain and the insert region of a GTPase may interact with different downstream targets; for example, the Rac insert region has been implicated in the activation of NADPH oxidase but not of PAK65 (17). RhoE may therefore interact with common RhoA effectors via its conserved effector domain but with different targets via its insert helix. Alternatively, as single point mutations inside the effector domains of Rac and Cdc42 can alter their interaction with different targets (24), subtle differences in or around the effector domains of RhoE and RhoA could alter effector specificity. Identification of downstream targets of RhoE will provide insights into the signalling pathways regulating stress fiber formation.

MDCK cells are highly motile in the presence of HGF/SF, spreading over the first 4 to 6 h after stimulation and then scattering as a consequence of cell-cell detachment (48). The dynamic assembly and disassembly of actin filaments provide the driving force for cell motility (13, 25, 31), and inhibitors of actin polymerization, such as cytochalasin B, prevent the scattering of MDCK cells (44). RhoE by itself did not mimic HGF/SF, in contrast to the rapid effect of activated H-Ras resembling HGF/SF-induced spreading (41), although it did induce some spreading in the long term. In the presence of HGF/SF, however, RhoE-injected cells showed an increase in migration speed. Similarly, RhoE induced an increase in the migration rate of R4.2 human mammary epithelial cells. Interestingly, previous studies suggested that highly motile or transformed cells have few stress fibers (8, 10, 28) and that a high level of stress fibers induced by RhoA inhibits HGF/SF motility (41). It is likely, therefore, that the RhoE-induced disappearance of stress fibers is responsible for the observed enhancement in migration.

As in MDCK cells, the microinjection of RhoE into Bac1.2F5 macrophages led to actin reorganization: cells extended broad, web-like actin-containing structures linking filopodium-like structures or smaller pseudopodia among longer and more numerous filopodium-like structures. This phenotype is clearly different from that observed in MDCK cells but may reflect a common mechanism for inhibiting RhoA signalling. In cells such as fibroblasts, RhoA is required to maintain a spread morphology by stimulating the attachment of stress fibers to focal adhesion sites (42). However, in cells that do not contain stress fibers, such as monocytes or macrophages and neuronal cells, RhoA is involved in maintaining cell tension and a round morphology (1, 2, 21). Microinjection of RhoA into Bac1.2F5 macrophages results in cell contraction and a more rounded appearance, whereas microinjection of C3 transferase into Bac1.2F5 macrophages leads to cell flattening and radial spreading (2). This response to C3 transferase is distinct from the morphology induced by RhoE, possibly, as described above, because RhoE only partially inhibits RhoA signalling. Interestingly, however, treatment of human monocytes and monocytic cell lines with C3 transferase leads to cell spreading with filopodial and pseudopodial extensions (1), resembling the RhoE-induced morphology in Bac1.2F5 cells.

The downstream targets of RhoE are not known yet, but its intracellular localization suggests where it is likely to exert its biological function. Three-dimensional reconstructions of confocal images showed that aggregates containing RhoE and actin are localized at the basal surfaces of MDCK cells, suggesting that they represent disrupted stress fibers. This localization may be similar to that reported for RhoE in osteosarcoma cells, where RhoE was observed in punctate structures distinct from focal adhesions (16). The localization of RhoE at the lateral membranes of MDCK cells suggests a role in cell-cell adhesion. Since RhoA is required to form adherens junctions in keratinocytes and MDCK cells (7, 50, 54), it would be interesting to determine if RhoE regulates junction formation or acts to inhibit RhoA signalling at this level. RhoE also appeared to localize to microvilli, suggesting that it could be involved in maintaining these actin-containing structures. In Bac1.2F5 macrophages, RhoE was associated with membrane ruffles, as has been reported for RhoA (49); this localization of RhoE is also consistent with its acting to antagonize RhoA.

Ruffles, cell-cell adhesion sites, and microvilli are specialized regions where actin filaments are linked to the plasma membrane. Recently, several studies have linked Rho to the ezrin/moesin/radixin family of proteins, which are implicated in actin filament-plasma membrane association (30, 51). Further studies focusing on the possible colocalization of ezrin/moesin/radixin proteins and RhoE should provide more information on the role of RhoE in regulating actin organization.

ACKNOWLEDGMENTS

We are grateful to Ritu Garg for excellent cell culture assistance, to Robert Harris and Thomas Eichholtz (Glaxo Wellcome) for the gift of the R4.2 cell line, and to Alan Entwistle for assistance with confocal laser scanning microscopy and image processing. We thank Emma Cannell for characterizing the r13, r15, r16, and r20 clones, Nick Totty for laser desorption mass spectrometric analysis of recombinant RhoE, and Jeff Settleman for advice and discussion of results. We also thank Ignacio Perez-Roger for help with the sequence analysis software.

This work was supported by European Communities grant ERBCH BGCT940702.

ADDENDUM IN PROOF

After submission of this paper, the sequences of *Rho6*, *Rho7*, and *Rho8* were published (C. D. Nobes et al., J. Cell Biol. **141:**1–11, 1998) and were renamed *Rnd*1, *Rnd*2, and *Rnd*3, respectively. The protein encoded by *Rnd*3 is identical to RhoE, except that it has an extra 15 amino acids at the N terminus.

REFERENCES

1. **Aepfelbacher, M., M. Essler, E. Huber, A. Czech, and P. C. Weber.** 1996. Rho is a negative regulator of human monocyte spreading. J. Immunol. **157:**5070–5075.
2. **Allen, W. E., G. E. Jones, J. W. Pollard, and A. J. Ridley.** 1997. Rho, Rac and Cdc42 regulate actin organization and cell adhesion in macrophages. J. Cell Sci. **110:**707–720.
3. **Amano, M., M. Ito, K. Kimura, Y. Fukata, K. Chihara, T. Nakano, Y. Matsuura, and K. Kaibuchi.** 1996. Phosphorylation and activation of myosin by Rho-associated kinase (Rho-kinase). J. Biol. Chem. **271:**20246–20249.
4. **Boguski, M. S., and F. McCormick.** 1993. Proteins regulating Ras and its relatives. Nature **366:**643–654.
5. **Boocock, C. A., G. E. Jones, E. R. Stanley, and J. W. Pollard.** 1989. Colony-stimulating factor-1 induces rapid behavioural responses in the mouse macrophage cell line, BAC1.2F5. J. Cell Sci. **93:**447–456.
6. **Bourne, H. R., D. A. Sanders, and F. McCormick.** 1991. The GTPase superfamily: conserved structure and molecular mechanism. Nature **349:**117–127.
7. **Braga, V. M., L. M. Machesky, A. Hall, and N. A. Hotchin.** 1997. The small GTPases Rho and Rac are required for the establishment of cadherin-dependent cell-cell contacts. J. Cell Biol. **137:**1421–1431.
8. **Bretscher, A.** 1991. Microfilament structure and function in the cortical cytoskeleton. Annu. Rev. Cell Biol. **7:**337–374.
9. **Burridge, K., and M. Chrzanowska Wodnicka.** 1996. Focal adhesions, contractility, and signaling. Annu. Rev. Cell Dev. Biol. **12:**463–518.
10. **Burridge, K., K. Fath, T. Kelly, G. Nuckolls, and C. Turner.** 1988. Focal adhesions: transmembrane junctions between the extracellular matrix and the cytoskeleton. Annu. Rev. Cell Biol. **4:**487–525.
11. **Chihara, K., M. Amano, N. Nakamura, T. Yano, M. Shibata, T. Tokui, H. Ichikawa, R. Ikebe, M. Ikebe, and K. Kaibuchi.** 1997. Cytoskeletal rearrangements and transcriptional activation of c-fos serum response element by Rho-kinase. J. Biol. Chem. **272:**25121–25127.
12. **Chrzanowska-Wodnicka, M., and K. Burridge.** 1996. Rho-stimulated contractility drives the formation of stress fibers and focal adhesions. J. Cell Biol. **133:**1403–1415.
13. **Cooper, J. A.** 1991. The role of actin polymerization in cell motility. Annu. Rev. Physiol. **53:**585–605.
14. **Dowrick, P. G., A. R. Prescott, and R. M. Warn.** 1991. Scatter factor affects major changes in the cytoskeletal organization of epithelial cells. Cytokine **3:**299–310.
15. **Entwistle, A., and M. Noble.** 1994. Optimizing the performance of confocal point scanning laser microscopes over the full field of view. J. Microsc. **175:**238–251.
16. **Foster, R., K. Q. Hu, Y. Lu, K. M. Nolan, J. Thissen, and J. Settleman.** 1996. Identification of a novel human Rho protein with unusual properties: GTPase deficiency and in vivo farnesylation. Mol. Cell. Biol. **16:**2689–2699.
17. **Freeman, J. L., A. Abo, and J. D. Lambeth.** 1996. Rac "insert region" is a novel effector region that is implicated in the activation of NADPH oxidase, but not PAK65. J. Biol. Chem. **271:**19794–19801.
18. **Hart, P. A., and C. J. Marshall.** 1990. Amino acid 61 is a determinant of sensitivity of rap proteins to the ras GTPase activating protein. Oncogene **5:**1099–1101.
19. **Hirshberg, M., R. W. Stockley, G. Dodson, and M. R. Webb.** 1997. The crystal structure of human rac1, a member of the rho-family complexed with a GTP analogue. Nat. Struct. Biol. **4:**147–152.
20. **Ishizaki, T., M. Naito, K. Fujisawa, M. Maekawa, N. Watanabe, Y. Saito, and S. Narumiya.** 1997. p160ROCK, a Rho-associated coiled-coil forming protein kinase, works downstream of Rho and induces focal adhesions. FEBS Lett. **404:**118–124.
21. **Jalink, K., E. J. van Corven, T. Hengeveld, N. Morii, S. Narumiya, and W. H. Moolenaar.** 1994. Inhibition of lysophosphatidate- and thrombin-induced neurite retraction and neuronal cell rounding by ADP ribosylation of the small GTP-binding protein Rho. J. Cell Biol. **126:**801–810.
22. **Kimura, K., M. Ito, M. Amano, K. Chihara, Y. Fukata, M. Nakafuku, B. Yamamori, J. Feng, T. Nakano, K. Okawa, A. Iwamatsu, and K. Kaibuchi.** 1996. Regulation of myosin phosphatase by Rho and Rho-associated kinase (Rho-kinase). Science **273:**245–248.
23. **Kozma, R., S. Ahmed, A. Best, and L. Lim.** 1995. The Ras-related protein Cdc42Hs and bradykinin promote formation of peripheral actin microspikes and filopodia in Swiss 3T3 fibroblasts. Mol. Cell. Biol. **15:**1942–1952.
24. **Lamarche, N., N. Tapon, L. Stowers, P. D. Burbelo, P. Aspenstrom, T. Bridges, J. Chant, and A. Hall.** 1996. Rac and Cdc42 induce actin polymerization and G1 cell cycle progression independently of p65PAK and the JNK/SAPK MAP kinase cascade. Cell **87:**519–529.
25. **Lauffenburger, D. A., and A. F. Horwitz.** 1996. Cell migration: a physically integrated molecular process. Cell **84:**359–369.
26. **Leung, T., X. Q. Chen, E. Manser, and L. Lim.** 1996. The p160 RhoA-binding kinase ROK α is a member of a kinase family and is involved in the reorganization of the cytoskeleton. Mol. Cell. Biol. **16:**5313–5327.
27. **Leung, T., E. Manser, L. Tan, and L. Lim.** 1995. A novel serine/threonine kinase binding the Ras-related RhoA GTPase which translocates the kinase to peripheral membranes. J. Biol. Chem. **270:**29051–29054.
28. **Lloyd, A. C., H. F. Paterson, J. D. Morris, A. Hall, and C. J. Marshall.** 1989. p21H-ras-induced morphological transformation and increases in c-myc expression are independent of functional protein kinase C. EMBO J. **8:**1099–1104.
29. **Machesky, L. M., and A. Hall.** 1996. Rho: a connection between membrane receptor signalling and the cytoskeleton. Trends Cell Biol. **6:**304–310.
30. **Mackay, D. J., F. Esch, H. Furthmayr, and A. Hall.** 1997. Rho- and rac-dependent assembly of focal adhesion complexes and actin filaments in permeabilized fibroblasts: an essential role for ezrin/radixin/moesin proteins. J. Cell Biol. **138:**927–938.
31. **Mitchison, T. J., and L. P. Cramer.** 1996. Actin-based cell motility and cell locomotion. Cell **84:**371–379.
32. **Morgan, C., J. W. Pollard, and E. R. Stanley.** 1987. Isolation and characterization of a cloned growth factor dependent macrophage cell line, BAC1.2F5. J. Cell. Physiol. **130:**420–427.
33. **Narumiya, S., T. Ishizaki, and N. Watanabe.** 1997. Rho effectors and reorganization of actin cytoskeleton. FEBS Lett. **410:**68–72.
34. **Nishiyama, T., T. Sasaki, K. Takaishi, M. Kato, H. Yaku, K. Araki, Y. Matsuura, and Y. Takai.** 1994. rac p21 is involved in insulin-induced membrane ruffling and rho p21 is involved in hepatocyte growth factor- and 12-O-tetradecanoylphorbol-13-acetate (TPA)-induced membrane ruffling in KB cells. Mol. Cell. Biol. **14:**2447–2456.
35. **Nobes, C. D., and A. Hall.** 1995. Rho, rac, and cdc42 GTPases regulate the assembly of multimolecular focal complexes associated with actin stress fibers, lamellipodia, and filopodia. Cell **81:**53–62.
36. **O'Hare, M. J., M. G. Omerod, P. Monaghan, E. B. Lane, and B. A. Gusterson.** 1991. Characterisation in vitro of luminal and myoepithelial cells isolated from the human mammary gland by cell sorting. Differentiation **46:** 209–221.
37. **Pizon, V., P. Chardin, I. Lerosey, B. Olofsson, and A. Tavitian.** 1988. Human cDNAs rap1 and rap2 homologous to the Drosophila gene Dras3 encode proteins closely related to ras in the 'effector' region. Oncogene **3:**201–204.
38. **Postma, F. R., K. Jalink, T. Hengeveld, and W. H. Moolenaar.** 1996. Sphingosine-1-phosphate rapidly induces Rho-dependent neurite retraction: action through a specific cell surface receptor. EMBO J. **15:**2388–2392.
39. **Reynet, C., and C. R. Kahn.** 1993. Rad: a member of the Ras family overexpressed in muscle of type II diabetic humans. Science **262:**1441–1444.
40. **Ridley, A. J.** 1996. Rho: theme and variations. Curr. Biol. **6:**1256–1264.
41. **Ridley, A. J., P. M. Comoglio, and A. Hall.** 1995. Regulation of scatter factor/hepatocyte growth factor responses by Ras, Rac, and Rho in MDCK cells. Mol. Cell. Biol. **15:**1110–1122.
42. **Ridley, A. J., and A. Hall.** 1992. The small GTP-binding protein rho regulates the assembly of focal adhesions and actin stress fibers in response to growth factors. Cell **70:**389–399.
43. **Ridley, A. J., H. F. Paterson, C. L. Johnston, D. Diekman, and A. Hall.** 1992. The small GTP-binding protein rac regulates growth factor-induced membrane ruffling. Cell **70:**401–410.
44. **Rosen, E. M., L. Meromsky, I. Goldberg, M. Bhargava, and E. Setter.** 1990. Studies on the mechanism of scatter factor. Effects of agents that modulate intracellular signal transduction, macromolecule synthesis and cytoskeleton assembly. J. Cell Sci. **96:**639–649.
45. **Rubinfeld, B., W. J. Crosier, I. Albert, L. Conroy, R. Clark, F. McCormick, and P. Polakis.** 1992. Localization of the rap1GAP catalytic domain and sites of phosphorylation by mutational analysis. Mol. Cell. Biol. **12:**4634–4642.
46. **Self, A. J., and A. Hall.** 1995. Measurement of intrinsic nucleotide exchange and GTP hydrolysis rates. Methods Enzymol. **256:**67–76.
47. **Smith, D. S., and K. S. Johnson.** 1988. Single-step purification of polypeptides expressed in *E. coli* as fusions with glutathione S-transferase. Gene **67:**31–40.
48. **Stoker, M., and M. Perryman.** 1985. An epithelial scatter factor released by embryo fibroblasts. J. Cell Sci. **77:**209–223.
49. **Takaishi, K., T. Sasaki, T. Kameyama, S. Tsukita, S. Tsukita, and Y. Takai.** 1995. Translocation of activated Rho from the cytoplasm to membrane ruffling area, cell-cell adhesion sites and cleavage furrows. Oncogene **11:**39–48.
50. **Takaishi, K., T. Sasaki, H. Kotani, H. Nishioka, and Y. Takai.** 1997. Regulation of cell-cell adhesion by Rac and Rho small G proteins in MDCK cells. J. Cell Biol. **139:**1047–1059.
51. **Tsukita, S., S. Yonemura, and S. Tsukita.** 1997. ERM proteins: head-to-tail regulation of actin-plasma membrane interaction. Trends Biochem. Sci. **22:** 53–58.
52. **Van Aelst, L., and C. D'Souza-Schorey.** 1997. Rho GTPases and signaling networks. Genes Dev. **11:**2295–2322.
53. **Wei, Y., Y. Zhang, U. Derewenda, X. Liu, W. Minor, R. K. Nakamoto, A. V. Somlyo, A. P. Somlyo, and Z. S. Derewenda.** 1997. Crystal structure of RhoA-GDP and its functional implications. Nat. Struct. Biol. **4:**699–703.
54. **Zhong, C., M. S. Kinch, and K. Burridge.** 1997. Rho-stimulated contractility contributes to the fibroblastic phenotype of Ras-transformed epithelial cells. Mol. Biol. Cell. **8:**2329–2344.
55. **Zhu, J., C. Reynet, J. S. Caldwell, and C. R. Kahn.** 1995. Characterization of Rad, a new member of Ras/GTPase superfamily, and its regulation by a unique GTPase-activating protein (GAP)-like activity. J. Biol. Chem. **270:** 4805–4812.